RADIOLOGICAL AND PHYSICO-CHEMICAL CHARACTERIZATION OF RED MUD AS AN Al-CONTAINING PRECURSOR IN INORGANIC BINDERS FOR THE BUILDING INDUSTRY

by

Ljiljana M. KLJAJEVIĆ [1*], ***Miljana M. MIRKOVIĆ*** [1], ***Sabina DOLENEC*** [2], ***Katarina ŠTER*** [2], ***Mustafa HADŽALIĆ*** [3], ***Ivana S. VUKANAC*** [4], ***and Miloš T. NENADOVIĆ*** [5]

[1]Department of Materials, Vinča Institute of Nuclear Sciences,
National Institute of the Republic of Serbia, University of Belgrade, Belgrade, Serbia
[2]Slovenian National Building and Civil Engineering Institute, Ljubljana, Slovenia
[3]University of Zenica – Institute Kemal Kapetanović, Zenica, Bosnia and Herzegovina
[4]Department of Radiation and Environmental Protection, Vinča Institute of Nuclear Sciences,
National Institute of the Republic of Serbia, University of Belgrade, Belgrade, Serbia
[5] Department of Atomic Physics, Vinča Institute of Nuclear Sciences,
National Institute of the Republic of Serbia, University of Belgrade, Belgrade, Serbia

Scientific paper
https://doi.org/10.2298/NTRP2002182K

The potential re-use of red mud in the building and construction industry has been the subject of research of many scientists. The presented research is a contribution to the potential solution of this environmental issue through the synthesis of potential construction materials based on red mud. A promising way of recycling these secondary raw materials is the synthesis of alkali-activated binders or alkali activated materials. Alkali-activated materials or inorganic binders based on red mud are a new class of materials obtained by activation of inorganic precursors mainly constituted by silica, alumina and low content of calcium oxide. Since red mud contains radioactive elements like ^{226}Ra and ^{232}Th, this may be a problem for its further utilization. The content of naturally occurring radionuclides in manufactured material products with potential application in the building and construction industry is important from the standpoint of radiation protection. Gamma radiation of the primordial radionuclides, ^{40}K and members of the uranium and thorium series, increases the external gamma dose rate. However, more and more precedence is being given to limiting the radiological dose originating from building materials on the population these days. The aim of this research was to investigate the possible influence of alkali activation-polymerization processes on the natural radioactivity of alkali activated materials synthesized by red mud (BOKSIT a. d. Milići, Zvornik, Bosnia and Herzegovina) and their structural properties. This research confirmed that during the polymerization process the natural radioactivity was reduced, and that the process of alkali activation of raw materials has an influence on natural radioactivity of synthesized materials.

Key words: red mud, inorganic binder, DRIFT, natural radioactivity, gamma index, building industry

INTRODUCTION

Red mud (RM) is a by-product of the alumina production process, which is produced by the processing of bauxite by the Bayer method. It is usually deposited in special locations in the form of a high-alkaline suspension. The amount of produced RM is increasing daily, and its disposal is a potential environmental hazard. Improper storage of bauxite residue can lead to harmful contamination of water, land and air in the surrounding area because of its high alkalinity. Strong environmental concerns are linked to the disposal of bauxite residue. The treatment and utilization of bauxite residue is both of environmental and economic significance. The global growth of bauxite residue highlights the urgency to develop and implement improved means of storage and remediation, and utilization options of its residue as an industrial by-product [1].

During the last two decades, extensive work has been done to develop various processes for utilization of RM by researchers in various areas: as special cements [2], in the ceramic industry [3], in ceramic glazes [4], in the aluminum industries by producing glasses and glass-ceramics, as an additive for construction materials [5], as the raw meal for the production of Portland cement clinker and in the production of heavy clay ceramics [6].

In this work, the inorganic binder's (IB) synthesis from a RM of Bosnia and Herzegovina – BOKSIT a.d.

* Corresponding author; e-mail: ljiljana@vin.bg.ac.rs

Table 1. Chemical composition of red mud expressed in oxide

Sample	wt. %										
	SiO_2	Al_2O_3	Fe_2O_3	CaO	MgO	Cr_2O_3	P_2O_5	K_2O	Na_2O	TiO_2	LoI
BHRM	12.08	15.04	48.08	7.26	0.43	0.13	0.19	0.05	7.47	4.88	4.39

Milići, (BHRM) by alkaline activation with a sodium silicate solution has been carried out. The changes in phase compositions and chemical-physical properties and micro-structure during the alkali activation process or reaction from the starting material to the final materials, IB based on BHRM (IBBHRM) have been followed to understand the formation of alkali activated binders. The synthesis is similar to an organic condensation polymerization [7]. In an alkaline environment, aluminum oxide and silicon oxide are dissolved from the solid precursor and form aluminate ($Al(OH)_4^-$) and silicate ([SiOx(OH)y]z-). The major silicate species are $[SiO(OH)_3]$- and $[SiO_2(OH)_2]^{2-}$ [8]. The following condensation reaction between aluminate and silicate is a nucleophilic substitution reaction. The monomers in a nucleophilic substitution react to form an aluminate silicate oligomer, from which an amorphous polymer is produced. This polymer forms a gel which subsequently hardens [9]. The oligomers undergo a further condensation reaction and release the water which was consumed during the hydrolysis.

The aim of this research was to investigate the possible influence of alkali activation processes on the natural radioactivity of aluminosilicate materials by gamma spectrometry measurements. In order to assess the radiological risk to human health it is important to measure the concentration of radionuclides in RM and obtained alkali activated RM samples/IB, because of their potential use in the building industry as building materials. The presented research is a contribution to the potential solution of environmental protection through the synthesis of potential construction materials based on RM or applications of RM as Al-rich by-products in the building industry, considering that a review of the available reference literature has shown that no significant testing of this waste material exists.

MATERIALS AND METHODS

Physical and chemical characterization of the RM

The BHRM was supplied by BOKSIT a.d. Milići, Zvornik, Bosnia and Herzegovina. The alumina factory is located in the northeastern part of Republika Srpska, in the industrial zone of Zvornik, only a kilometer away from the river Drina and the border with Serbia. In this factory bauxite is processed into alumina. Most of the ore is procured from the nearby Boksit Milići mine, and a smaller part from the nearby mines in Vlasenica and Srebrenica, as well as from imports. The amount of total RM emitted from the alumina factory is estimated at over 10 000 000 tons.

The RM powder sample was ground after being dried at 105 ºC for 24 hours, for removal of the retained variable water in the RM. Table 1 shows the chemical composition of RM, as determined by X-ray fluorescence (XRF). The XRF analysis was performed with a wavelength dispersion (WD XRF) spectroscope ARL Perform X manufactured by Thermo Scientific with a power of 2500 W, 5 GN Rh X-ray tube, 4 crystals (AX03, PET, LiF200 and LiF220), two detectors (proportional and scintillation), and computer program UniQuant. The samples were quartered, dried at 105 ° C and calcined at 950 °C. For measurement purposes, a fused pellet was prepared, where 0.7640 g of the sample and 7.64 g of the flux (50 % lithium tetraborate versus 50 % lithium metaborate) were melted at 1100 ° C.

The X-ray powder diffraction (XRD) was performed to determine the phase composition of the RM sample using a PANalytical Empyrean X-ray diffractometer equipped with CuK radiation with λ = 1.54 A. 5 g of the samples were ground in an agate mortar to a particle size below 0.063 mm. The ground powder was manually back loaded into a circular sample holder (diameter 16 mm). The samples were scanned at 45 kV and a current of 40 mA, over the 2θ range from 4° to 70°, at a scan rate of 0.026° 2θ min^{-1} and step time 172 seconds. The obtained XRD patterns were analysed using X'Pert High Score Plus diffraction software v. 4.8 from PANalytical, using PAN ICSD v. 3.4 powder diffraction files. All Rietveld refinements were performed using the PANalytical X'Pert High Score Plus diffraction software, using the structures for the phases from ICDD PDF 4+ 2016 RDB powder diffraction files. Amorphous content was determined using the external standard method (NIST SRM 676a) [10]. Table 2 shows the quantitative content of the identified phase of the BHRM sample.

The Brunauer-Emmett-Teller (BET) specific surface area of the BHRM sample (pre-dried for 60 minutes at 105 °C) was performed with Micromeritics ASAP-2020 that integrates multiple gas sorption techniques into a single, convenient tabletop instrument). The bulk density of BHRM was determined according to standard JUS B.C8.023 and moisture content (removal of all the water but chemically bound water)

Table 2. Quantitative contents of the identified phase of the BHRM sample

BHRM	Phase [%]				
	Amorphous	Hematite	Cancrinite	Calcite	Kaolinite
	43.2	21.1	18.3	0.9	16.5

Table 3. Surface area, specific and bulk density, moisture content of the investigated sample

Sample	BET surface area [m^2g^{-1}]	Specific density [gcm^{-3}]	Bulk density [$kgdm^{-3}$]	Moisture content [%]
BHRM	12.9	2.35	755	0.23

was determined by drying the sample in an oven SP-440 (maximum T 300 °C) on 105 °C for 24 hours. Moisture content is given with the equation

$$mcwb = [(Ww - Wd)/Ww] \times 100\ [\%]$$

where mc is expressed on a wet basis (Ww is the wet weight and Wd is the dry weight).

Table 3 shows the surface area, specific and bulk density, moisture content of BHRM.

Synthesis of alkali activated materials or inorganic binder based on RM

The IB were prepared by using sodium silicate solutions (the content of Na_2O and SiO_2 was 12.3 % and 22.5 %, respectively) provided by Galenika Magmasil d.o.o (Belgrade, Serbia), and 12M NaOH solution (NaOH, Sigma – Aldrich). The volume ratio of the solution of NaOH and sodium silicate solution was 1.5, while the liquid to solid (L/S) mass ratio was 1.0, and it is dependent on an acceptable workability for the paste sample.

The waste BHRM as the solid component and the alkali silicate activator were mixed until a homogenous slurry was formed. The prepared pastes were cast in cylindrical molds (diameter/height, 100 mm/80 mm) and compacted on a vibrating table. The molds were closed to avoid water evaporation and stored at room temperature 24 hours, after that 72 hours in an oven at a temperature of 60 °C, and after that at room temperature for 28 days. The reaction occurs at 60 °C temperature and is activated by a highly alkaline solution, and forms, amorphous polymers and the binding phase in these synthesized materials is a tetrahedrally coordinated alkali-aluminosilicate gel.

Characterization of RM and inorganic binder

Samples of BHRM and IBBHRM were ground in a porcelain mortar and manually loaded in a monocrystalline silicon sample holder (square shaped 1 cm 1 cm) and characterized by XRD analysis using the Ultima IV Rigaku diffractometer, equipped with Cu $K_{1,2}$ radiation, with generator voltage 40.0 kV and generator current 40.0 mA. The range of 5°-80° 2θ was used for all powders in a continuous scan mode with a scanning step size of 0.02° at a scan rate of 5 ° min^{-1}. The PDXL2 software was used to evaluate the phase composition and identification of all samples [11]. All obtained patterns are compared using the ICDD data-base [12]. For phase identification PDF (powder diffraction file) card numbers are presented in the discussion part.

The functional group of all samples was determined by Diffuse reflectance infrared Fourier transform (DRIFT) spectroscopy. The DRIFT spectra were obtained using the Perkin-Elmer FTIR spectrometer Spectrum Two [13]. Approximately 5 % of the samples were dispersed in an oven-dried spectroscopic grade KBr with the refractive index of 1.559 and particle size of 5-20 m. The spectra were scanned at a 4 cm^{-1} resolution and collected in the mid-IR region from 4000 to 400 cm^{-1}.

The microstructure analysis was performed on an Au-coated surface of the samples using a Japan Electron Optics Laboratory electron microscope (JEOL JSM) 6390 LV at 25 kV coupled with Energy Dispersive X-Ray Spectroscopy (EDS), Oxford Instruments X-MaxN.

The contents of naturally occurring radionuclides in the samples were determined by gamma spectrometry. Prior to measurement, the samples were powdered and placed in PVC cylindrical containers (125 ml and 250 ml), sealed with beeswax and left for six weeks in order to reach radioactive equilibrium between radon and its progenies. Radiological analysis was performed by means of a coaxial semiconductor high purity germanium (HPGe) detector (Canberra 7229N-7500-1818 with 20 % relative efficiency and 1.8 keV resolution for ^{60}Co at the 1332 keV line) associated with standard beam supply electronics units. Measurements were performed in accordance with international recommendations [14]. Energy and efficiency calibration of the spectrometer was done based on laboratory standards prepared with a certified radioactive solution purchased from the Czech Metrology Institute [15] and traceable to the BIPM (Bureau International des Poids et Mesures). Obtained efficiencies were corrected for the coincidence summing effect using the correction factors obtained with EFTRAN software [16]. The samples were measured for 60 000 seconds. All spectra were recorded and analyzed using the Canberra's Genie 2000 software; net areas of the peaks were corrected for the background radiation. The obtained specific activities are given in tab. 3, expressed in $Bqkg^{-1}$. Quoted uncertainties (the confidence level of 1σ) were calculated by the error propagation calculation. The combined standard uncertainties included the statistical uncertainties of the recorded peaks, efficiency calibration uncertainty and the uncertainty of measured mass.

RESULTS AND DISCUSSION

The XRD analysis

Mineralogical composition of the RM depends on the mineral composition of the source material – bauxite, a multiphase ore that may contain more than a

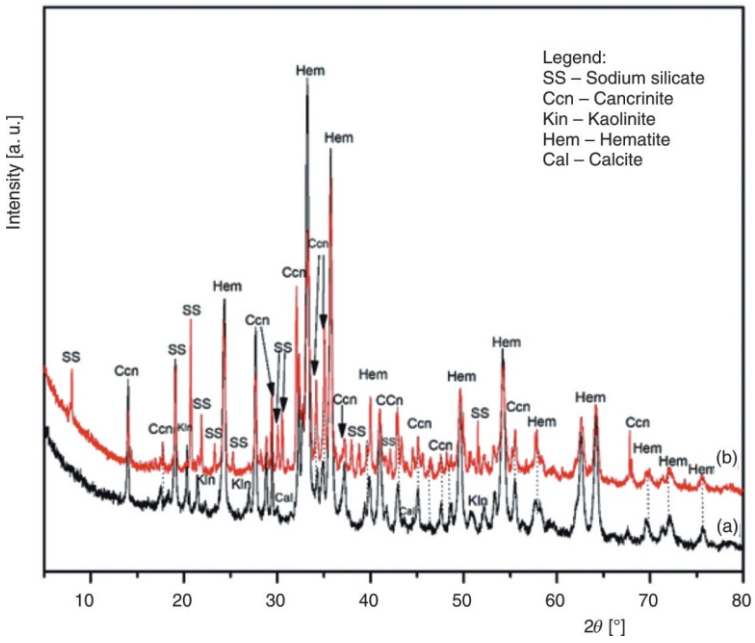

Figure 1. The XRD patterns of (a) BHRM, and inorganic binder based on BHRM and (b) IBBHRM

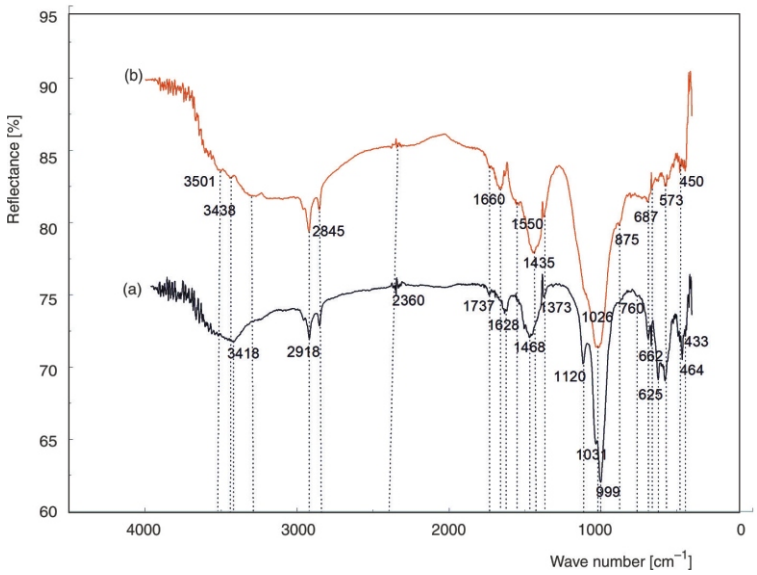

Figure 2. The DRIFT spectra of (a) BHRM, and inorganic binder based on BHRM and (b) IBBHRM

hundred minerals of various grinding fineness and decomposition [17]. The minerals containing of aluminum, iron, silicon, titanium, calcium, magnesium are essential constituents. Depending on the type of mineral deposits, the amounts of the essential and accessory minerals may vary within wide ranges [17, 18].

Figure 1 shows the XRD patterns of BHRM, and alkali activated materials – IBBHRM.

The main crystallographic phases detected in the BHRM sample are: hematite (PDF No. 01-089-8104), cancrinite (PDF No. 00-020-0257), kaolinite (PDF No 01-078-3262), and calcite (PDF No. 01-078-3262). Based on quantitative XRD analysis there is 43.2 % of the amorphous phase. The results of XRD analysis indicate that after the alkali activation process and structural rearrangement of minerals presented in raw materials there is a segregation of the sodium silicate hydrate phase with a corresponding chemical composition Na_2SiO_3 6 H_2O. Due to alkali activation and ageing process over time, this semi-crystalline sodium silicate phase separates. The mineralogical composition of alkali activated material consists of sodium silicate, cancrinite ($Na_6Ca_2Al_6Si_6O_{24}(CO_3)_2$) and hematite, while the calcite ($CaCO_3$) and kaolinite ($Al_2(OH)_4Si_2O_5$) peaks are not identified. This is in correlation with the alkali activation process because it leads to their dissolution in the silicate matrix activator.

Table 1 shows that the content of the Fe_2O_3 is analogous to the Spanish RM [19] and higher than in most of the cases reported in the literature. The hematite compound is interesting for industrial applications due to its ability to tune the color of ceramics by adjusting the RM content and the processing conditions. The presence of SiO_2 is also interesting since its reaction with the Na_2O and CaO present can lead to compounds with a lower melting temperature than the other com-

ponents of the sample. It would provide for a liquid phase in the grain boundaries, facilitating the sintering of these materials.

The DRIFT analysis

Figure 2 shows the DRIFT spectra of the BHRM (a), and IBBHRM (b). The spectra were compared to known absorption lines in literature.

The DRIFT spectra shown in fig. 2, related to BHRM and IBBHRM show thee wide band at region 3500-3400 cm^{-1} indicating the presence of the –OH stretching band. The absorption bands at 2918 cm^{-1} and 2845 cm^{-1} were related to asymmetric and symmetric aliphatic $–CH_2$ groups, respectively. The spectra also indicate the presence of $CaCO_3$, mainly in the form of calcite, as identified by its main absorption bands at about 1468 cm^{-1} and 875 cm^{-1}. The peak recorded at 1400 cm^{-1} (1373 cm^{-1}) in the BHRM and IBBHRM could be attributed to nitrate. This NO_3 band might be present in cancrinite, according to the results reported by Zhao *et al*. 2004 [20]. The peaks near 1031 cm^{-1} and 999 cm^{-1} were derived from in-plane Si-O stretching modes and the former was the most intense kaolinite band. The bands near 760 cm^{-1} and 687 cm^{-1} were both associated with perpendicular Si–O vibration. Al–O–Si and Si–O–Si bending vibrations produced the bands at 573 cm^{-1} and 464 cm^{-1}, respectively. The peak at 433 cm^{-1} corresponded to Si–O deformation vibration. A stretching vibration of Fe–O is observed in the region around 470 cm^{-1} [17].

There is a persistence of the bands at 3438 cm^{-1} and 1660 cm^{-1} in IBBHRM (assigned to hydroxyl groups coordinated with Al^{3+} cations), which are the stretching and bending vibrations for the hydroxyl groups of water molecules [21]. A band at 1435 cm^{-1} belongs to the O–C–O stretching vibration of the carbonate phase which is shifted to higher wavenumbers in relation to the RM. As a result of alkali activation some bands are shifted to a smaller or larger wavelength. The band around 1028 cm^{-1} corresponded to the Si–O stretching vibration [22]. The modification of the shape of the Si–O stretching band at around 1028 cm^{-1} indicates a change in the Si environment after alkali activation [21, 23]. Alkali activated BHRM present DRIFT spectra characterized by the typical absorption bands of Si–O–Si and Si–O–Al bonds (absorption range 600-800 cm^{-1}). One of the DRIFT signals that give information about the degree of alkali activation, is the band at 3450 cm^{-1} correlated to the chemically bonded water. This band is broad in the spectrum of IBBHRM, confirming the formation of the new material. Furthermore, the alkali activation induces a slight shift of the band of T–O–Si (T = Si, Al) stretching towards lower wavenumbers because of the formation of hydrogen bonds with hydroxyl groups present in the system compared to the same bonds in the spectrum of BHRM.

Moreover, in the BHRM and IBBHRM spectra, a band due to stretching vibrations of the Fe-O bond (460-500 cm^{-1}) was also present [24]. The DRIFT spectra of the BHRM and IBBHRM samples showed slight differences with respect to the untreated sample; in particular the band at 1120 cm^{-1} in BHRM spectra practically in the DRIFT spectra of IBBHRM did not appear. The results of DRIFT analysis are consistent with those obtained from the XRD analysis of BHRM and IBBHRM.

The SEM/EDS analysis

The SEM images with EDS analysis, fig. 3, show the morphology changes that occurred in the alkali activated RM sample. Morphological characteristics are an effective tool to assess the efficiency and ascertain the compatibility of a stabilizing agent. Furthermore, aggregation of particles by interlocking or bonding before and after alkali activation or solidification can be visualized only from the morphological studies [25].

Figure 3 reveals the fact that BHRM particles have a mixed morphology, with no prevailing particular shape form. The images show that the BHRM is composed of particles with a different shape (roundness and sphericity).

The sodium silicate gel was observed as the majority product, along with the unreacted particles of crystal phases present in alkali activated RM, during the aging time up to 28 days. The micro-structure was inhomogeneous and the matrix was full of loosely structured crystal grains of different sizes. Numerous pores of different shape size are evident in the gel. The considerable amount of unreacted particles and the presence of pores in the alkali activated matrix, fig. 3, indicate an incomplete alkali activated reaction of RM. If the silica content increases, the degree of reaction taking place in the forming paste decreases according to observations in reference [26]. The EDS analysis of alkali activated material, IBBHRM fig. 3(d) showed that it mostly consists of the phases containing Na, Si, Al in the bulk region suggesting the formation of a silicate-activated gel by polymerization throughout the inter particles volume. This correlates with the published works [27] meaning that, in a medium with a high concentration of dissolved silica, the species dissolved from the surface of the particles, migrate from the surface into the bulk solution. In addition, Fe, Al, Si, and Ca were also observed in the gel by EDS analysis fig. 3(d). These obviously represent the element of crystal phases, which did not dissolve during alkali activation. During alkaline activation these crystal phases may even disperse through the gel.

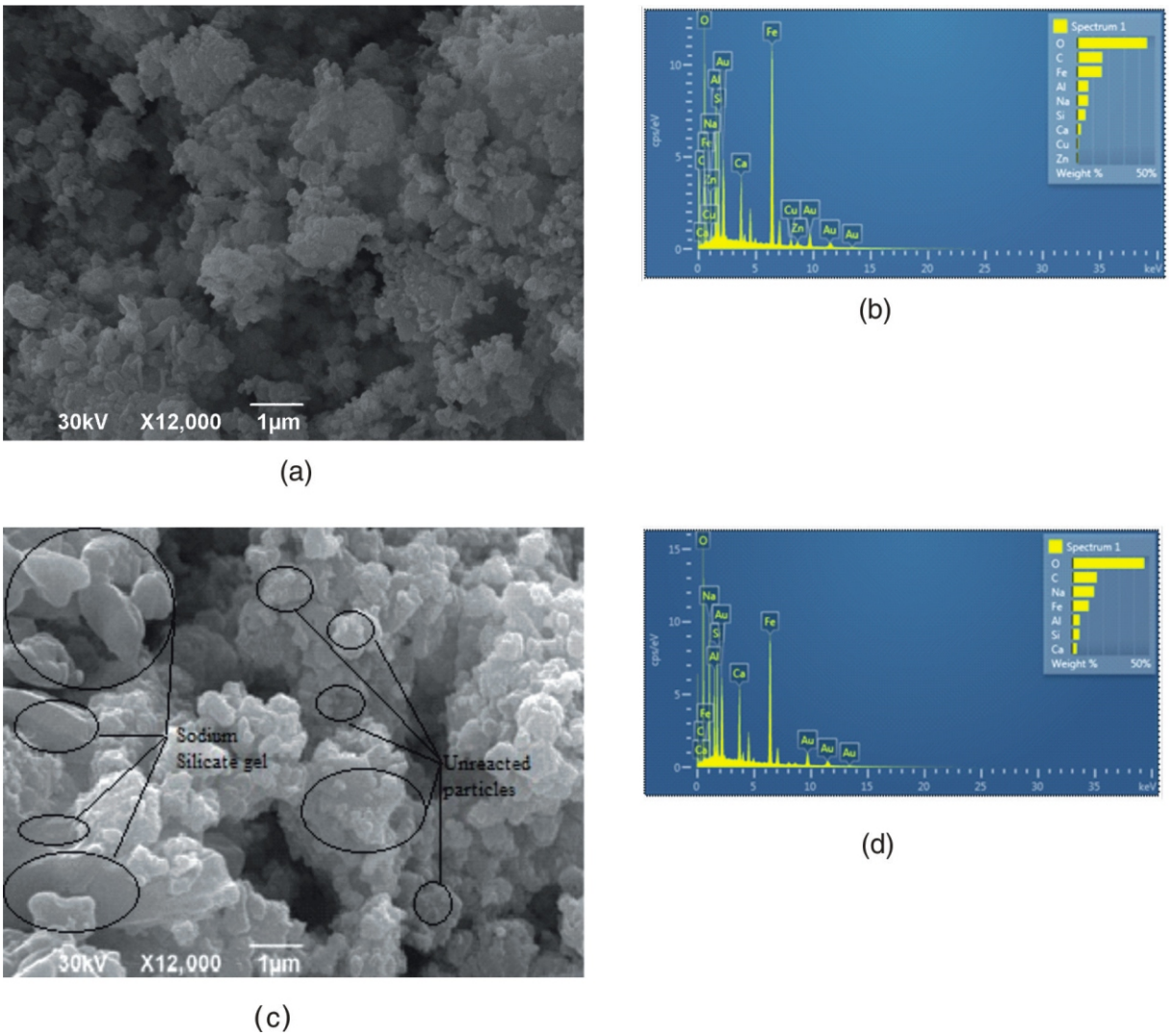

Figure 3. The SEM images with EDS analysis of (a) and (b) BHRM and (c) and (d) IBBHRM

Table 4. Activity concentration of natural radionuclides and ^{137}Cs in investigated samples with associated measurement uncertainties (k = 1)

	Specific activity [Bqkg^{-1}]		Activity ratio
	BHRM	IBBHRM	IBBHRM/BHRM
^{210}Pb	107 11	74 12	0.69 0.13
^{212}Pb	386 27	171.7 23.1	0.45 0.07
^{214}Pb	188 12	94.0 7.2	0.50 0.05
^{12}Bi	426 29	200.8 23.6	0.47 0.06
^{214}Bi	168 9	85.1 7.1	0.51 0.05
^{226}Ra	176 7	91 6	0.52 0.04
^{232}Th	397 25	187 15	0.47 0.05
^{40}K	32 6	<17	
^{137}Cs	<0.1	<0.4	
^{238}U	164 15	72 17	0.44 0.11
^{235}U	10.3 1.5	4.0 0.5	0.39 0.07
$^{235/238}$U	0.067	0.057	
Gamma index	2.58	1.24	

Radiological analysis

Results of gamma spectrometric analysis are given in tab. 4, and based on obtained specific activities of ^{226}Ra, ^{232}Th, and ^{40}K dose calculations were performed. The ratio of activities is also presented. The calculated ratio is approximately 0.5 for all detected radionuclides. To a certain extent this result could be explained by analyzing the masses of constituents of newly formed material and the synthesis process itself.

Natural radioactivity of various building materials has been reported by researchers in many countries such as China, Egypt, Israel, Pakistan, Lebanon, Greece, North Macedonia, Serbia, Turkey, and Austria *etc*. [28]. World average ^{232}Th, ^{226}Ra, and ^{40}K activity concentrations for building materials are 50 Bqkg^{-1}, 50 Bqkg^{-1}, and 500 Bqkg^{-1}, respectively [17].

In order to assess whether the safety requirements for building materials are being fulfilled, a gamma activity concentration index (abbreviation

ACI is often used in literature) proposed by the European Commission [29] was used. It is defined as,

$$I \quad \frac{A_{Ra}}{300\,Bqkg^{-1}} \quad \frac{A_{Th}}{200\,Bqkg^{-1}} \quad \frac{A_{K}}{3000\,Bqkg^{-1}} \quad (1)$$

where A_{Ra}, A_{Th}, and A_K are the specific activities of ^{226}Ra, ^{232}Th, and ^{40}K, respectively. The index I is correlated with the annual dose rate due to the excess external gamma radiation caused by a superficial material. The limit values depend on the dose criteria, the way and amount of the material and the manner in which it was used in a building and construction. For material used in bulk amounts I 1 corresponds to an absorbed gamma dose rate of 1 mSv per year [29, 30]. The activity concentration index should be used only as a screening tool for identifying materials that might be of concern for use as construction materials. The European Commission [29] suggests that building materials should be exempt from all restrictions concerning their radioactivity provided the excess gamma radiation originating from them does not increase the annual effective dose to a member of the public by more than 0.3 mSv [31, 32]. An annual dose higher than 1 mSv should be permitted only in some very exceptional cases where materials are used locally.

Besides the activity concentration index, in order to estimate a possible health effect due to the exposure to natural radionuclides present in the measured samples, radium equivalent activity, Ra_{eq} [Bqkg^{-1}], the external hazard index, H_{ex} [Bqkg^{-1}], total external absorbed gamma dose rate $\dot{D}$ [nGyh^{-1}], and annual effective dose *EDR* [mSv] can be calculated. The radium equivalent activity can be used to estimate the hazard associated with materials that contain ^{226}Ra, ^{232}Th, and ^{40}K. The external radiation hazard index reflects the external radiation hazard due to the emitted gamma radiation. The values of these indicators of exposure can be calculated according to eqs. (2) and (3), [33-35].

$$Ra_{eq} \quad A_{Ra} \quad 1.43A_{Th} \quad 0.017A_{K} \quad (2)$$

$$H_{ex} \quad \frac{A_{Ra}}{370} \quad \frac{A_{Th}}{259} \quad \frac{A_{K}}{4180} \quad (3)$$

If the examined materials are treated as a possible raw material for building material or construction material itself, different formulae should be used for dose calculation. Using the formulae given in [29], the external dose rate and annual effective dose rate are calculated as eqs. (4) and (5), respectively.

$$\dot{D} \quad 0.92A_{Ra} \quad 1.1A_{Th} \quad 0.08A_{K} \quad (4)$$

$$EDR(\text{mSv}) \quad \dot{D}(\text{nGyh}^{-1}) \quad 7000\,\text{h} \quad 0.7(\text{SvGy}^{-1})10^{-6} \quad (5)$$

Table 5 presents the calculated values of the radium equivalent activity, Ra_{eq}, radiation hazards, H_{ex}, absorbed dose rate, $\dot{D}$, and annual effective dose rate, *EDR* of BHRM and IBBHRM, and those given in the literature.

Results showed that the significantly higher values of specific activities as well as for calculated parameters were obtained for raw materials. The lowest values were observed for the synthesized materials.

Thus, regarding its radioactivity the investigated synthetized materials could be recommended as a promising construction material, or its component. In Serbian legislation the gamma index has to be calculated for building materials [36] and its components, in order to estimate whether or not they could be used as building materials. For these components, especially for materials originating from industrial activities, representing waste, the factor of the share in the final material must be taken into account [37].

This research confirmed that during the polymerization process the natural radioactivity was reduced, *i. e.*, the process of raw materials activation has an influence on natural radioactivity of synthesized materials. Also, Bošković *et al.* [17], concluded that after alkaline activation of RM, the decrease of specific radioactivity was measured in comparison to RM as raw materials [18]. The obtained results have given the guidance for further optimization of the polymerization process in order to confirm and explain changes in radioactivity concentrations.

CONCLUSIONS

New IB based on the RM sample supplied by *BOKSIT* a.d. Milići, Zvornik, Bosnia and Herzegovina, BHRM were synthetized. Physico-chemical characterization of BHRM and IBBHRM was conducted using

Table 5. Radium equivalent activity, external radiation hazard index, external absorbed dose rate, annual effective dose rate, and gamma index

Sample	Ra_{eq} [Bqkg^{-1}]	H_{ex} [Bqkg^{-1}]	$\dot{D}$ [nGyh^{-1}]	*EDR* [mSv]	I	Reference
	Measured in this study					
BHRM	746.2	2.016	601.2	2.946	2.58	Our research
IBBHRM	358.4	0.968	289.4	1.418	1.24	Our research
Mean value, previous studies						
Almasfuzito RM – Hungary	706.9	1.91	306.1	0.375	2.44	[18]
Ajka RM – Hungary	901.1	2.43	399.6	0.490	3.07	[18]
RM – Montenegro	778.1	2.104	623.8	3.057	2.75	[17]
Geopolymer RM – Montenegro	208.9	0.578	177.6	0.870	0.6	[17]

XRD and DRIFTS. Based on quantitative XRD analysis there is 43.2 % of the amorphous phase. The results showed that the amorphous phases were dissolved and that a gel is produced, which is identified by SEM/EDS analysis. Interpretation of DRIFT results is more complex. The movement of certain DRIFT peaks, as well as the appearance of new ones and the disappearance of some originated from the starting RM indicate the development of new materials. The use of RM and alkali activated materials based on RM in the construction industry requires very strict assessments which includes physico -chemical characterization and radiological consideration. Radiological testing is necessary in assessing whether the existing material meets all legal regulations in order to be used as a building material. Results of the presented study confirmed our previous results [38, 39] that values of radiological indicators decrease during the process of synthesis of new materials. Since this material is investigated for potential use in the construction sector, the obtained results are very promising from the point of view of optimizing the external exposure of the population to ionizing radiation originating from gamma emitters from surrounding building materials.

ACKNOWLEDGMENT

This work was financially supported by the Ministry of Education, Science and Technological Development of the Republic of Serbia (Contract no. 451-03-9/2021-14/ 200017) and also, has received funding from the European Institute of Innovation and Technology (EIT), a body of the European Union, under Horizon 2020, the EU Framework Programme for Research and Innovation (RIS-ALiCE , project no. 18258).

This research did not receive any specific grant from funding agencies in the public, commercial, or not-for-profit sectors.

Authors would like to thank Dr. Snežana S. Nenadović, Vinča Institute of Nuclear Sciences- National Institute of the Republic of Serbia, University of Belgrade, Belgrade, Serbia and Dr. Lea Žibert, Slovenian National Building and Civil Engineering Institute, Ljubljana, Slovenia for their contribution in realization of research presented in this manuscript.

AUTHORS' CONTRIBUTIONS

Lj. M. Kljajević and M. T. Nenadović conceptualized the research, designed and prepared the research plan, synthesized the samples, and revised the manuscript. M. Hadžalić selected and characterized sample of RM. I. S. Vukanac performed radionuclide studies in the samples, analyzed the obtained data. M. M. Mirković contributed in analyzing of the XRD results. S. Dolenec and K. Šter performed some physico-chemical analysis of the samples. All the authors contributed to the literature research, data analysis and the preparation of the manuscript.

REFERENCES

[1] Power, G., *et al*., Bauxite Residue Issues: I. Current Management, Disposal and Storage Practices, *Hydrometallurgy, 108* (2011), 1-2, pp. 33-45
[2] Singh, M., *et al*., Preparation of Special Cements from RM, *Waste Manag, 16* (1996), 8, pp. 665-670
[3] Sglavo, M., *et al*., Bauxite 'RM' in the Ceramic Industry, Part I. Thermal behaviour, *J Eur Ceram Soc, 20* (2000), 3, pp. 235-244
[4] Yalci, N., Sevinc, V., Utilization of Bauxite Waste in Ceramic Glazes, *Ceram Int, 26* (2000), 5, pp. 485- 493
[5] Pan, Z., *et al*., Properties and Microstructure of the Hardened Alkali-Activated Bauxite RM Slag Cementitious Material, *Cem Concr Res, 33* (2003), pp. 1437-1441
[6] Pontikes, Y., *et al*., Thermal Behavior of Clay Mixtures with Bauxite Residue for the Production of Heavy Clay Ceramics, *J Eur Ceram Soc, 27* (2007), 2-3, pp. 1645-1649
[7] Yao, X., *et al*., Geopolymerization Process of Alkali-Metakaolinite Characterized by Isothermal Calorimetry, *Thermochim Acta, 493* (2009), 1-2, pp. 49-54
[8] Weng, L., *et al*., Effects of Aluminates on the Formation of Geopolymers, *Mater Sci Engn B, 117* (2005), 2, pp. 163-168
[9] Provis, J. L., *et al*., The Role of Mathematical Modelling and Gel Chemistry in Advancing Geopolymer Technology*, Chem Eng Res Des, 83* (2005), 7, pp. 853-860
[10] Cline, J. P., *et al*, Addressing the Amorphous Content Issue in Quantitative Phase Analysis: the Certification of NIST Standard Reference Material 676a, *Acta Cryst, A67* (2011), pp. 357-367
[11] ***, Rigaku, PDXL Integrated X-Ray Powder Diffraction Softvare, 2.8.4.0. ed: Rigaku, Tokyo; 2011
[12] ***, International Crystallographical Database (ICDD), in: N.S. 12 Campus Blvd, Pann., 19073, USA (Ed.) USA, 2012
[13] Griffiths, P. R., de Haseth, J. A., *Fourier Transform Infrared Spectrometry*, 2nd Edition, John Wiley & Sons Publisher, New York, USA, 2007, pp 349-361
[14] ***, IAEA, Measurement of Radionuclides in Food and the Environment, Technical Report Series, No 295, 1989, Vienna, Austria
[15] ***, CMI, Radioactive Standard Solutions, ER X, Cert. no. 1035-SE-40844-17, 2017, Czech Metrology Institute, Prague,Czechia
[16] Vidmar, T., EFFTRAN-A Monte Carlo Efficiency Transfer Code for Gamma-Ray Spectrometry, Nucl. Instrum, *Methods Phys Res Sect A, 550* (2005), 3, pp. 603-608
[17] Bošković, V. I., *et al*., Radiological and Physicochemical Properties of RM Based Geopolymers, *Nucl Technol Radiat, 3*3 (2018), 2, pp. 188-194
[18] Nenadović, S. S., *et al*., Physicochemical, Mineralogical and Radiological Properties of RM Samples as Secondary Raw Materials, *Nucl Technol Radiat, 32* (2017), 3, pp. 261-266
[19] Pascual, J., *et al*., Thermal Characterization of a Spanish RM, *J Therm Anal Calor, 96* (2009), 2, pp. 407-412
[20] Zhao, H. T., *et al*., Alteration of Kaolinite to Cancrinite and Sodalite by Simulated Hanford Tank Waste and Its Impact on Cesium Retention, *Clays Clay Miner, 52* (2004), 1, pp. 1-13

[21] Tyagi, B., *et al*., Determination of Structural Modification in Acid Activated Montmorillonite Clay by FT-IR Spectroscopy, Spectrochim, *Acta Part A, 64* (2006), 2, pp. 273-278
[22] Madejova, J., Komadel, P., Baseline Studies of the Clay Minerals Society Source Clays: Infrared Methods, *Clays Clay Miner, 49* (2001), October, pp. 410-432
[23] Gervais, F., *et al*., Infrared Reflectivity Spectroscopy of Silicate Glasses, *J Non-Cryst Solids, 89* (1987), 3, pp. 384-401
[24] Mozgawa, W., *et al*., MAS NMR and FTIR Spectra of Framework Aluminosilicates, *J Molec Structure, 614* (2002), 1-3, pp. 281-287
[25] De Silva, P., *et al*., Kinetics of Geopolymerization: Role of Al_2O_3 and SiO_2, *Cem Concr Res, 37* (2007), 4, pp. 512-518
[26] Provis, J. L., van Deventer, J. S. J., Direct Measurement of the Kinetics of Geopolymerisation by In-Situ Energy Dispersive X-Ray Diffractometry, *J Mate. Sci, 42* (2007), Dec., pp. 2974-2981
[27] Lee, W. K. W., van Deventer, J. S. J., Structural Reorganisation of Class F Fly Ash in Alkaline Silicate Solutions, *Colloids Surf A Physicochem Eng Asp, 211* (2002), 1, pp. 49-66
[28] Zhuang, S., Lu, X., Natural Radio Activity and Radiological Hazard of Red-Clay Brick Produced in Shangluo, China, *Nucl Technol Radiat, 35* (2020), 4, pp. 347-353
[29] ***, EC, Radiation Protection 112, Radiological Protection Principles Concerning the Natural Radioactivity of Building Materials, European Commission, Luxembourg, (1999), ISBN 92-828-8376-0
[30] Stojanovska, Z., *et al*., Natural Radioactivity and Human Exposure by Raw Materials and end Product from Cement Industry Used as Building Materials, *Radiat Meas, 45* (2010), 8, pp. 969-972
[31] Righi, S., Bruzzi, L., Natural Radioactivity and Radon Exhalation in Building Materials Used in Italian Dwellings, *J Environ Radioact, 88* (2006), 2, pp. 158-170
[32] Ravisankar, R., *et al*., Determination of Natural Radioactivity and the Associated Radiation Hazards in Building Materials Used in Polur, Tiruvannamalai District, Tamilnadu, India Using Gamma Ray Spectrometry with Statistical Approach, *J Geoch Explor, 163* (2016), April, pp. 41-52
[33] O'Brien, R. S., Cooper, M. B., Technologically Enhanced Naturally Occurring Radioactive Material (NORM): Pathway Analysis and Radiological Impact, *Appl Radiat Isot, 49* (1998), 3, pp. 227-239
[34] Mulwa, B. M., *et al*., Radiological Analysis of Suitability of Kitui South Limestone for use as Building Material, *Int J Fundam Phys Sci, 3* (2013), 2, pp. 32-35
[35] Ajayi, J. O., *et al*., Assessment of Radiological Hazard Indices of Building Materials in Ogbomoso, South-West Nigeria, *Environ Nat Resources Research, 3* (2013), 2, pp. 128-132
[36] ***, Rulebook on the Limits on the Content of Radionuclides in Drinking Water, Foodstuffs, Animal Feed, Medicines, General Use, Construction Materials and Other Goods Placed on the Market ("Official Gazette of the Republic of Serbia" No. 36 Dated 10.05.2018)
[37] Vukanac, I., *et al*., Assessment of Natural Radioactivity Levels and Radon Exhalation Rate Potential from Various Building Materials, *Nucl Technol Radiat 35* (2020), 1, pp. 64-73
[38] Ivanović, M., *et al*., Physicochemical and Radiological Characterization of Kaolin and its Polzmerization Products, *Mater de Construction, 68* (2018), 330, pp. 1-10
[39] Nenadović, S., *et al.*, Chemical, Physical and Radiological Evaluation of Raw Materials and Geopolymers for Building Applications, *J Radioanal Nuc Chem, 325* (2020), June, pp. 435-445

Received on June 24, 2021
Accepted on August 16, 2021

Љиљана М. Кљајевић, Миљана М. Мирковић, Сабина Доленец, Катарина Штер, Мустафа Хаџалић, Ивана С. Вуканац, Милош Т. Ненадовић

РАДИОЛОШКА ПРОЦЕНА ЦРВЕНОГ МУЉА КАО Al-ПРЕКУРСОРА НЕОРГАНСКИХ ВЕЗИВА ЗА ГРАЂЕВИНСКУ ИНДУСТРИЈУ

Потенцијална поновна употреба црвеног муља у грађевинској индустрији била је предмет истраживања многих научника. Приказана истраживања доприносе могућем решењу овог еколошког питања кроз синтезу потенцијалних грађевинских материјала на бази црвеног муља. Обећавајући начин рециклирања ових секундарних сировина је синтеза алкално активираних везива или алкално активираних материјала. Алкално активирани материјали или неорганска везива на бази црвеног муља су нова класа материјала добијених активацијом неорганских прекурсора који се углавном састоје од силицијум диоксида, алуминијум диоксида и ниског садржаја калцијум оксида. Будући да црвени муљ садржи радиоактивне елементе попут ^{226}Ra и ^{232}Th, то може представљати проблем за његово даље коришћење. Садржај природних радионуклида у произведеним материјалима са потенцијалном применом у грађевинарству важан је са становишта заштите од зрачења. Гама зрачење примордијалних радионуклида, ^{40}K и чланова серије уранијума и торијума, повећава спољну дозу гама зрачења. Међутим, све се више у данашње време даје приоритет ограничавању радилошке дозе која потиче од грађевинског материјала на становништво. Циљ овог истраживања био је истражити могући утицај процеса алкативне активације-полимеризације на природну радиоактивност алкално активираних материјала синтетисаних употребом црвеног муља (“БОКСИТ” а. д. Милићи, Зворник) и њихових структурних својстава. Ово истраживање потврдило је да је током процеса полимеризације смањена природна радиоактивност, тако да процес алкалне активације сировине утичу на природну радиоактивност синтетизованих материјала.

Кључне речи: црвени муљ, неорганска везива, DRIFT, природна радиоактивност, гама индекс, грађевинарство